New phases in CP-violating B decay asymmetries from mixing to singlet down quarks

Woon-Seng Choong and Dennis Silverman
Department of Physics, University of California, Irvine, Irvine, California 92717
(Received 16 August 1993)

Groups such as E_6 with extra $SU(2)_L$ singlet down quarks give rise to flavor-changing neutral currents (FCNC's) through the mixing of four or more down quarks. These currents may substantially contribute to the processes of B_d^0-$\bar{B}_d^0$ and B_s^0-$\bar{B}_s^0$ mixing, within the allowed range of nonzero values for the four quark mixing parameters. These would then introduce new angles and phases into the CP-violating B decay asymmetries. Other, negative FCNC experiments put limits on these angles. Using a maximum likelihood analysis with contributions from both the standard model and the FCNC's, we find large regions for new physics phases contributing to CP-violating B decay asymmetries. From the bound on the mixing elements, the new singlet down quark might have a mass above the 500 GeV range.

PACS number(s): 14.40.Nd, 11.30.Er, 11.30.Ly, 12.15.Mm

I. INTRODUCTION

Groups such as E_6 with extra $SU(2)_L$ singlet down quarks give rise to flavor-changing neutral currents (FCNC's) through the mixing of four or more down quarks [1]. These FCNC's with Z^0-mediated exchange may contribute to part of B_d^0-$\bar{B}_d^0$ mixing [2] and of B_s^0-$\bar{B}_s^0$ mixing, giving a range of nonzero values for the fourth quark's mixing parameters. If these are a large contributor to the B_d-$\bar{B}_d$ mixing, they introduce new angles into the CP-violating B decay asymmetries. The size of the contribution of the FCNC amplitude U_{db} to the unitarity triangle is bounded to be less than 0.05 of the unit base, but we find that it can contribute as large an amount to B_d-$\bar{B}_d$ mixing as does the standard model. We find that the new phases can appear in this mixing as well as in B_s -$\bar{B}_s$ mixing, and give phases completely different from that of the standard model in CP-violating B decay asymmetries.

FCNC experiments put limits on these new mixing angles that constrain the possibility of new physics accounting for B_d^0-$\bar{B}_d^0$ and B_s^0-$\bar{B}_s^0$ mixing. In an earlier paper [3] we analyzed the constraints on the mixing angles analytically but approximately, and formed a plot of the FCNC amplitude $|U_{db}|$ versus $|V_{td}|$ which showed an allowed region for FCNC's dominating B_d^0-$\bar{B}_d^0$ mixing. In this paper we analyze jointly all constraints on a 4×4 mixing matrix obtained by assuming only one of the $SU(2)_L$ singlet down quarks mixes appreciably. We use the experiments used on the 3×3 Cabibbo-Kobayashi-Maskawa (CKM) submatrix elements [4] which include those on the six matrix elements $V_{ud}, V_{cd}, V_{us}, V_{cs}, V_{ub}, V_{cb}$ of the u and c quark rows, and, in the neutral K system, include $|\epsilon|$, $K_L \to \mu\mu$ (for which there are two experiments), and also B_d-$\bar{B}_d$ mixing. In this paper studying FCNC's, we add the $B \to \mu\mu X$ bound (which constrains $b \to d$ and $b \to s$), Δm_K (which constrains $s \to d$ along with the other K experiments), and $Z^0 \to b\bar{b}$ (which directly constrains the V_{4b} quark mixing element). We analyze all of these together using a joint χ^2 for fitting all of the 13 experiments in the nine-parameter angle space of the 4×4 mixing matrix. We include both the standard model and FCNC contributions through effective Hamiltonians. We then make a maximum likelihood plot for $|U_{db}|$ versus the magnitude of the competing standard model amplitude $|U_{\rm std}|$ which is proportional to $|V_{td}|$. Plots are also made for the phase difference of the combined amplitude for B_d-$\bar{B}_d$ mixing minus the standard model phase, versus the phase of the standard model amplitude alone, which show that almost any phase can occur through new physics to be observed in CP-violating B_d^0 decay asymmetries. Similar conclusions follow for B_s-$\bar{B}_s$ mixing, only with a smaller allowed region of new phases.

There are an additional five parameters in the four-quark mixing matrix above those present in the three-quark CKM [5] matrix, namely, three new angles and two new phases, and there are essentially seven experiments on FCNC to set limits on their magnitudes and phases. Experiments limit combined phases in U_{ds} and somewhat in U_{db}. If the FCNC does contribute significantly to B_d^0-$\bar{B}_d^0$ mixing, this phase, along with the detection of the other FCNC, will be needed for a complete determination of the 4×4 angles. The B_d^0-$\bar{B}_d^0$ mixing sets the best limit on $|U_{db}|$. The $B \to \mu\bar{\mu}X$ limit on $|U_{db}|$ is much weaker, but it sets the best limit on $|U_{sb}|$. The small 2.4% error on $\Gamma(Z^0 \to b\bar{b})$ bounds the mixing matrix element $|V_{4b}|$. Also, the very small 0.2% error on $|V_{us}|$ and similar error on $|V_{ud}|$ with the normalization of the u quark row set similar stringent limits on $|V_{4b}|$. Then, $K_L \to \mu\bar{\mu}$ bounds $|\mathrm{Re}(U_{ds})|$, the $K_L - K_S$ mass difference bounds $\mathrm{Re}[(U_{ds})^2]$ and thereby effectively $|\mathrm{Im}(U_{ds})|$, and ϵ bounds $|\mathrm{Im}[(U_{ds})^2]|$ giving a bound on the product $2|\mathrm{Re}(U_{ds})\mathrm{Im}(U_{ds})|$. In first examining each experiment separately, we will give indicative bounds as if the FCNC acted alone, but in the χ^2 and maximum likelihood analysis, we consider all possible contributions of the standard model and FCNC parts.

In Sec. II we formulate the down quark mixing fla-

vor changing neutral currents. With Z^0 exchange to the FCNC we construct effective Hamiltonians in Sec. III. In Secs. IV, V, and VI we apply bounds from $B \to \mu\mu X$, B_d-$\bar{B}_d$ mixing, and $Z^0 \to b\bar{b}$, respectively. In Sec. VII we apply bounds on U_{ds} from K meson short distance physics. In Sec. VIII we convert to the angles in the 4×4 mixing matrix, and examine their contribution to B_d-$\bar{B}_d$ mixing through U_{db} in Sec. IX. In Sec. X is described the limits on the angles from graphically examining χ^2 surfaces in the nine-parameter space. In Sec. XI the maximum likelihood method is used to construct minimum χ^2 plots in pairs of physical amplitudes and phases for B_d-$\bar{B}_d$ and B_s-$\bar{B}_s$ mixing. We also examine the maximum likelihood limits on the new mixing matrix elements. In Sec. XII we present maximum likelihood plots for corrections to unitarity triangles. In Sec. XIII we present an estimate of a lower bound on the mass of the first singlet quark and briefly discuss its production mechanisms. In Sec. XV we summarize our conclusions.

II. FLAVOR-CHANGING NEUTRAL CURRENTS FROM MIXING

We use a basis where the three up quark states are the mass eigenstates. In the down quark sector we mix in a fourth down quark which is an $SU(2)_L$ singlet, and use the 4×4 matrix V which diagonalizes the initial down quarks (d^0_{iL}) to the mass eigenstates (d_{jL}) by $d^0_{iL} = V_{ij} d_{jL}$. The combination of the diagonal matrix in the up quarks and the matrix V give the charged current interactions

$$\mathcal{L} = \frac{g}{\sqrt{2}}(W^-_\mu J^{\mu+} + W^+_\mu J^{\mu-}), \tag{1}$$

$$J^{\mu-} = \bar{u}_{iL}\gamma^\mu d^0_{iL} = V_{ij}\bar{u}_{iL}\gamma^\mu d_{jL}, \tag{2}$$

where here $i = 1,2,3$ and $j = 1,2,3,4$. Here the 3×4 submatrix of V couples the three up quarks to the four down quarks. The 3×3 submatrix of V for $i,j = 1,2,3$ takes the role of the CKM matrix for mixing the standard model quarks, but it is not unitary by itself.

The weak isospin part of the three $SU(2)_L$ doublet quarks can be written in terms of all four quarks by using a 4×4 t_3 matrix such that $(t_3)_{44} = 0$:

$$\mathcal{L} = \frac{e}{\sin\theta_W \cos\theta_W} \bar{d}^0_{kL}(t_3)_{km} d^0_{mL}, \tag{3}$$

$$(t_3)_{km} = -\frac{1}{2}\delta_{km} + \frac{1}{2}\delta_{k4}\delta_{4m}. \tag{4}$$

Converting to mass eigenstates by $d^0_{mL} = V_{mj} d_{jL}$ and $\bar{d}^0_{kL} = V^*_{ki}\bar{d}_{iL}$ gives

$$\mathcal{L}^Z = \frac{e}{\sin\theta_W \cos\theta_W} V^*_{ki} V_{mj} \bar{d}_{iL}(t_3)_{km} d_{jL}. \tag{5}$$

The flavor-changing neutral currents ($i \neq j$) are given by the $\delta_{k4}\delta_{4m}$ term in $(t_3)_{km}$:

$$\mathcal{L}^Z_{\text{FCNC}} = -\frac{e}{2\sin\theta_W \cos\theta_W} U_{ij}\bar{d}_{iL}\gamma^\mu d_{jL} Z_\mu, \tag{6}$$

with amplitudes [6]

$$-U_{ij} \equiv V^*_{4i} V_{4j} \quad \text{for} \quad i \neq j. \tag{7}$$

The diagonal neutral current couplings are reduced in strength by the amplitudes into the FCNC, becoming, when $i = j$,

$$\mathcal{L}^Z_{\text{NC}} = -\frac{e}{2\sin\theta_W \cos\theta_W} \sum_i (1 - |V_{4i}|^2)\bar{d}_{iL}\gamma^\mu d_{iL} Z_\mu. \tag{8}$$

FCNC experiments will bound the three amplitudes U_{ds}, U_{sb}, and U_{bd} which contain three new mixing angles and three phases.

III. FCNC EFFECTIVE HAMILTONIAN

The FCNC processes with Z^0 exchange would contribute at the same time as the second-order weak neutral current flavor-changing processes in the standard model. At the FCNC tree level of a four-fermion effective Hamiltonian, for quarks coupling to muon pairs, the FCNC's couple to a virtual Z^0 created in the neutral current annihilation channel. In the four-quark effective Hamiltonian, the FCNC contribute through tree level Z^0 exchange as well, and both annihilation and exchange graphs contribute the same. This is the same as in the standard model box diagrams for four-quark couplings. We can then add the FCNC Z^0 exchange terms to the standard model second-order weak four-fermion effective Hamiltonian H_{eff}, as computed by Inami and Lim [7], and carry them along in all treatments of H_{eff} applied to various neutral current processes (see also [8] and [9]).

The four-quark neutral current effective Hamiltonian for s and d quarks from Inami and Lim [7], and from using Eq. (6) in the two tree level Z exchange diagrams of equal magnitude (and dividing by 2×2 for having two choices for s and d fields),

$$H^{4q}_{\text{eff}} = \frac{G_F}{\sqrt{2}}(\bar{d}_L\gamma_\mu s_L)^2 \left\{ \frac{\alpha}{4\pi\sin^2\theta_W}(-\tilde{E}^*) + U^2_{ds} \right\}. \tag{9}$$

For K meson processes, $-\tilde{E}^*$ becomes [10], with QCD corrections ($y_c = m_c^2/m_W^2$),

$$-\tilde{E}^* = \eta_1 (V^*_{cd}V_{cs})^2 y_c + \eta_2 (V^*_{td}V_{ts})^2 y_t f_2(y_t) + 2\eta_3 (V^*_{cd}V_{cs}V^*_{td}V_{ts}) y_c f_3(y_t). \tag{10}$$

The K^0-$\bar{K}^0$ mixing matrix element is

$$\langle K^0 | [\bar{d}\gamma_\mu(1-\gamma_5)s]^2 | \bar{K}^0 \rangle = \tfrac{4}{3} f_K^2 m_K^2 B_K \tag{11}$$

and $f_K = \sqrt{2}F_K = 165$ MeV. The value of the coefficient of the standard model result versus U^2_{ds} in Eq. (9) is small (as are the terms in $-\tilde{E}^*$):

$$\frac{\alpha}{4\pi\sin^2\theta_W} = 2.5 \times 10^{-3}. \tag{12}$$

For the $K_L \to \mu\mu$ semileptonic effective Hamiltonian we have from Inami and Lim [7] and from the FCNC tree level virtual Z^0 exchange,

$$H_{\rm eff}^{ds} = \frac{G_F}{\sqrt{2}}\bar{s}\gamma_\mu(1-\gamma_5)d\bar{\mu}\gamma^\mu(1-\gamma_5)\mu\left[-\frac{\alpha\tilde{C}}{4\pi\sin^2\theta_W} - \frac{1}{2}U_{sd}\right], \tag{13}$$

where

$$\tilde{C} = V_{cs}^* V_{cd} y_c + \tfrac{1}{4}V_{ts}^* V_{td} y_t \left| 1 + 3/(1-y_t) + 3y_t \ln y_t/(1-y_t)^2 \right| . \tag{14}$$

Additional vector terms do not contribute to $K_L \to \mu\mu$ since the meson matrix element gives P_K^μ which vanishes on the vector muon current.

For $B \to \mu\mu X$ we drop the standard model terms since they give a result which is less than one-third of the 1σ bounds [11]. We thus use this experimental result from UA1 [11] only to give bounds on FCNC Z^0-mediated processes with the $H_{\rm eff}^{bd+bs}$:

$$H_{\rm eff}^{bd+bs} = \frac{G_F}{\sqrt{2}}\left[U_{bd}\bar{b}\gamma_\mu(1-\gamma_5)d + U_{bs}\bar{b}\gamma_\mu(1-\gamma_5)s\right] \times\left[-\frac{1}{2}\bar{\mu}\gamma^\mu(1-\gamma_5)\mu + 2\sin^2\theta_W\bar{\mu}\gamma^\mu\mu\right]. \tag{15}$$

IV. BOUND FROM $B \to \mu\mu X$

The Z-mediated process forms μ pairs from the FCNC $b \to d$ and $b \to s$ with amplitudes U_{db} and U_{sb}, respectively. The ratio of these rates to the W-mediated semileptonic decay is

$$\frac{B(B\to\mu\mu X)}{B(B\to\mu\nu X)} = \left[(1/2-\sin^2\theta_W)^2 + (\sin^2\theta_W)^2\right] \times\frac{|U_{db}|^2+|U_{sb}|^2}{|V_{ub}|^2+F_{ps}|V_{cb}|^2}; \tag{16}$$

where $F_{ps} \simeq 0.5$.

The new bound from UA1 at 1σ (reduced from 5×10^{-5} at 90% C.L. by 1.64) is [11]

$$B(B\to\mu\mu X) < 3\times10^{-5}, \tag{17}$$

which when scaled by the branching ratio for the W-mediated decay to $\mu\nu$ of 0.103 bounds the ratios [12]

$$\left|\frac{U_{db}}{V_{cb}}\right| < 0.034, \quad \left|\frac{U_{sb}}{V_{cb}}\right| < 0.034. \tag{18}$$

This new bound is an improvement by a factor of 5 on the $|U_{qb}|$ from the previous bounds from this process. With the values $|V_{cb}| = 0.043$, the range of the bounds on U_{db} and U_{sb} are

$$|U_{db}| \le 0.0015, \quad |U_{sb}| \le 0.0015. \tag{19}$$

With the normalization in Eq. (6) relative to the flavor-nonchanging neutral currents, the above bounds lead to predictions of less than two flavor-changing b-$\bar{s}$ or b-$\bar{d}$ or their charge conjugate decays out of $Z^0 \times 10^6$ decays.

V. B_d-$\bar{B}_d$ MIXING

Mixing may occur by the b-$\bar{d}$ quarks in a $\bar{B}_d$ annihilating to a virtual Z through a FCNC with amplitude U_{db}, and the Z then creating $\bar{b}$-d quarks through another FCNC, which then becomes a B_d meson.

For B_d-$\bar{B}_d$ mixing, the analogous $H_{\rm eff}$ to Eq. (9) for four-quark b-d coupling gives

$$x_d = \frac{2G_F}{3\sqrt{2}}B_B f_B^2 m_B \eta_B \tau_B \left|\frac{\alpha}{4\pi\sin^2\theta_W} y_t f_2(y_t)(V_{td}^* V_{tb})^2 + (U_{db})^2\right|, \tag{20}$$

where $x_d = \Delta m_{B_d}/\Gamma_{B_d} = \tau_{B_d}\Delta m_{B_d} = \tau_{B_d} 2|M_{12}|$.

The experimental and calculated parameters are [10]

$$x_d = 0.66 \pm 0.11, \tag{21}$$

$$\tau_b|V_{cb}|^2 = (3.5\pm0.6)\times10^9\ {\rm GeV}^{-1}, \tag{22}$$

$$\sqrt{B_B}f_B = 0.220 \pm 0.040\ {\rm GeV}, \tag{23}$$

$$\eta_B = 0.55, \tag{24}$$

where we have used the new and larger lattice value [13] for $\sqrt{B_B}f_B$ and for consistency, the next to leading order η_B [14].

To orient to the magnitude of the terms, requiring that FCNC alone account for the observed value of B_d^0-$\bar{B}_d^0$ mixing would result in $|U_{db}/V_{cb}| = 0.016$, which with 1σ limits is

$$0.009 < \left|\frac{U_{db}}{V_{cb}}\right| < 0.022. \tag{25}$$

Thus the B_d^0-$\bar{B}_d^0$ mixing by Z-mediated FCNC, above, is still well allowed by the new bound on $B \to \mu\mu X$, Eq. (18), where $|U_{db}/V_{cb}| \le 0.034$. Using the central value of V_{cb} this gives an indicative central value for the FCNC amplitude if acting alone of

$$|U_{db}| = 0.0007. \tag{26}$$

VI. BOUND FROM $Z^0 \to b\bar{b}$

The reduction in the diagonal neutral current coupling for $Z^0 \to b\bar{b}$ by the factor $(1-|V_{4b}|^2)$ allows a constraint from the CERN e^+e^- collider LEP data. The theoretical decay rate for $Z^0 \to b\bar{b}$ including this FCNC reduction is

$$V^b = -\tfrac{1}{2}(1-|V_{4b}|^2) + \tfrac{2}{3}\sin^2\theta_W + \tfrac{1}{3}\rho_t, \tag{27}$$

$$A^b = -\tfrac{1}{2}(1-|V_{4b}|^2) + \tfrac{1}{3}\rho_t, \tag{28}$$

$$C_{\rm QCD} = 3(1.0385), \tag{29}$$

$$\Gamma^{\rm std+FCNC}(Z^0\to b\bar{b}) = \frac{C_{\rm QCD}G_F m_Z^3}{6\sqrt{2}\pi}\left[(V^b)^2+(A^b)^2\right], \tag{30}$$

where $\rho_t = 0.0072$ for $m_t = 150$ GeV. The ratio of $Z^0 \to b\bar{b}$ to the standard model, for small $|V_{4b}|^2$, is

$$\frac{\Gamma_{b\bar{b}}^{\text{std+FCNC}}}{\Gamma_{b\bar{b}}^{\text{std}}} = (1 - 2.29|V_{4b}|^2). \tag{31}$$

Recent analysis of LEP data [15] shows an increase by either about 1σ or 0.3σ for the ratio of experiment to the standard model using either a general analysis of a few experiments or all LEP experiments with standard model assumptions, respectively. With this ambiguity, as well as the fact that a true positive result would be due to a different effect, we use only a zero deviation result with a 2.4% error, giving a χ^2,

$$\chi^2 = \left(\frac{2.29|V_{4b}|^2}{0.024}\right)^2. \tag{32}$$

This gives the 1σ and 2σ limits

$$|V_{4b}| \leq 0.10, \quad |V_{4b}| \leq 0.14, \tag{33}$$

respectively. This bound shows up as the maximum $|V_{4b}|$ below in the minimum χ^2 plots (see Fig. 4).

VII. FCNC BOUNDS FROM *K* MESON PHYSICS

K meson physics gives bounds on the real part of U_{ds} and on the real and imaginary parts of U_{ds}^2.

A. Short distance contribution to $K_L \to \mu\mu$

Combining the new results for the branching ratio for $K_L \to \mu\mu$ from BNL [16] of $(6.86 \pm 0.37) \times 10^{-9}$ and from KEK [17] of $(7.9 \pm 0.7) \times 10^{-9}$ gives

$$B(K_L \to \mu\mu) = (7.09 \pm 0.33) \times 10^{-9}, \tag{34}$$

with an added χ^2 for the fit of 1.7. The result from the 2γ intermediate state is [18] $(6.83 \pm 0.28) \times 10^{-9}$. The 2γ absorptive contribution is purely imaginary, while the K_L superposition isolates the real part from the standard model and the FCNC Z-mediated decays. Bounding the difference of the rates as being due to the real part gives

$$|A_R|^2 = (0.26 \pm 0.43) \times 10^{-9}. \tag{35}$$

The short distance (SD) contribution to the branching ratio is

$$\frac{B(K_L^{SD} \to \mu\mu)}{B(K^+ \to \mu^+\nu_\mu)} = \frac{\tau_{K_L}}{\tau_{K^+}|V_{us}|^2}\left|\frac{\alpha}{2\pi \sin^2\theta_W}\text{Re}(\tilde{C}) + \text{Re}(U_{ds})\right|^2. \tag{36}$$

If the difference were due to the FCNC amplitude alone, the relation is

$$|A_R|^2 = 54[\text{Re}(U_{ds})]^2. \tag{37}$$

Using the difference plus 1σ error as an upper bound on $|A_R|^2 \leq 0.69 \times 10^{-9}$ gives the indicative bound

$$|\text{Re}(U_{ds})| \leq 2.6 \times 10^{-5}. \tag{38}$$

B. $K_L - K_S$ mass difference

The Z-mediated FCNC also contribute to the neutral K meson mass difference. The long distance contribution may range from zero to 50% of the mass difference. The standard model and FCNC short distance contribution is

$$\Delta m_K(1 - D) = \Delta m_K^{\text{SD}} = 2|M_{12}^{\text{SD}}| = \frac{2G_F m_K B_K f_K^2}{3\sqrt{2}}\left|\frac{\alpha}{4\pi \sin^2\theta_W}\text{Re}(-\tilde{E}^*) + \text{Re}(U_{ds}^2)\right|, \tag{39}$$

with the experimental result being

$$\Delta m_K = 3.52 \times 10^{-15} \text{ GeV}. \tag{40}$$

The first term in

$$\text{Re}(-\tilde{E}^*) = \eta_1 \text{Re}[(V_{cd}^* V_{cs})^2] y_c \tag{41}$$

dominates and is essentially fixed. The value of $B_K = 0.67 \pm 0.20$ corresponds to a short distance fraction $(1 - D) = 0.39 \pm 0.12$. We then use as a 1σ bound on the FCNC the order of the remainder or Δm_K. Requiring $(\Delta m_K)_{\text{FCNC}} \leq \Delta m_K$, the bound from this on the FCNC contribution is

$$|\text{Re}[(U_{ds})^2]| \leq 8.8 \times 10^{-8}. \tag{42}$$

This effectively gives

$$|\text{Im}(U_{ds})| \leq 3.0 \times 10^{-4}, \tag{43}$$

$$|U_{ds}| \leq 3.0 \times 10^{-4}. \tag{44}$$

C. Bounds on FCNC *CP* violation in $|\epsilon|$

The contributions of the four-quark H_{eff}^{4q}, Eq. (9), for the standard model and the FCNC Z^0 exchanges to $|\epsilon| = 2.27 \times 10^{-3}$ give the contribution

$$|\epsilon| = \frac{G_F f_K^2 B_K m_K}{12\Delta m_K}\left[\frac{\alpha}{4\pi \sin^2\theta_W}\text{Im}(-\tilde{E}^*) + \text{Im}(U_{ds}^2)\right]. \tag{45}$$

If this is applied as an upper bound to the FCNC part alone, the indicative result (for $B_K = 2/3$) is

$$|\text{Im}[(U_{ds})^2]| \leq 9.2 \times 10^{-10}. \tag{46}$$

This effectively gives

$$|\text{Re}(U_{ds})\text{Im}(U_{ds})| \leq 4.6 \times 10^{-10}. \tag{47}$$

VIII. BOUNDS ON MIXING ANGLES

We consider the up quark basis as being diagonal in the up quark masses, up to phases. Despite having three up quarks with the four down quarks, the down quarks still mix with a 4×4 unitary matrix, and the extra phases can be removed by shifting the relative down and up quark phases, and the fourth row can still have its relative phase changed, even though there is no fourth up quark to which it couples. We thus use the standard CKM-like 4×4 matrix [19]. This holds for one new singlet down quark, but not beyond. For a rigorous derivation, see [20]. All cosine terms in the 4×4 mixing matrix are near 1. For simplicity we show the leading terms in the matrix elements of V, in terms of the sines and cosines of the mixing angles, although in practice the calculations are done with exact elements [19]:

$$V = \begin{pmatrix} c_{12}c_{34} & s_{12}c_{34} & s_{13}e^{-i\delta_{13}} & s_{14}e^{-i\delta_{14}} \\ -s_{12} & 1 & s_{23} & s_{24}e^{-i\delta_{24}} \\ (s_{12}s_{23} - s_{13}e^{i\delta_{13}}) & -s_{23} & 1 & s_{34} \\ V_{4d} & V_{4s} & V_{4b} & c_{34} \end{pmatrix}. \tag{48}$$

The complex conjugates of the mixing matrix elements in the fourth row, keeping only leading terms in the new angles, are [19]

$$V_{4d}^* = -s_{14}e^{-i\delta_{14}} + s_{24}e^{-i\delta_{24}}s_{12} - s_{34}(s_{12}s_{23} - s_{13}e^{-i\delta_{13}}), \tag{49}$$

$$V_{4s}^* = -s_{24}e^{-i\delta_{24}} + s_{34}(s_{23} + s_{12}s_{13}e^{-i\delta_{13}}) - s_{14}e^{-i\delta_{14}}s_{12}, \tag{50}$$

$$V_{4b}^* = -s_{34} - s_{24}e^{-i\delta_{24}}s_{23} - s_{14}e^{-i\delta_{14}}s_{13}e^{i\delta_{13}}. \tag{51}$$

Using the bound on $\mathrm{Re}(U_{ds})$ above, for the four-quark mixing form $-U_{ij} = V_{4i}^* V_{4j}$, we get

$$|\mathrm{Re}(V_{4d}^* V_{4s})| \leq 2.6 \times 10^{-5}. \tag{52}$$

Having tight bounds on U_{ds} and U_{sb} we can ask if it is still consistent to have a value for U_{db} large enough to account for B_d-$\bar{B}_d$ mixing. We combine all three to get a bound on V_{4s} by first substituting in the definitions of the U's as follows:

$$-U_{db} = V_{4d}^* V_{4b} = \frac{U_{ds}}{V_{4s}} \frac{U_{sb}}{V_{4s}^*}. \tag{53}$$

We then substitute on the right the bounds on $|U_{ds}|$ and on $|U_{sb}/V_{cb}|$, and on the left the value of $|U_{db}|/|V_{cb}|$ to account for B_d-$\bar{B}_d$ mixing:

$$0.016 = |U_{db}/V_{cb}| \leq 3.0 \times 10^{-4} \times 0.034/|V_{4s}|^2, \tag{54}$$

which gives

$$|V_{4s}|^2 \leq 0.00064 \quad \text{or} \quad |V_{4s}| \leq 0.025. \tag{55}$$

If this restriction is satisfied, the two bounds above are consistent, and the matrix elements $|V_{4d}|$ and $|V_{4b}|$ can be large enough for U_{db} to account for a part of B_d-$\bar{B}_d$ mixing. (From Fig. 4 below, this is indeed the case.)

IX. PHASES IN *CP*-VIOLATING *B* DECAY ASYMMETRIES

The CP-violating decay asymmetries [21] rely on a relative phase between the B_d^0-$\bar{B}_d^0$ mixing and the b quark decay amplitudes into final states of definite CP. Since we have found that Z-mediated FCNC processes may contribute significantly to B_d^0-$\bar{B}_d^0$ mixing, the phases of U_{db} would be important. To leading order in s_{34}, $s_{24}e^{-i\delta_{24}}$, and $s_{14}e^{-i\delta_{14}}$ we have

$$U_{db} = -s_{34}(s_{34}V_{td}^* + s_{14}e^{-i\delta_{14}} - s_{24}e^{-i\delta_{24}}s_{12}). \tag{56}$$

We note that the first term has the same phase as in the standard model where the box diagram with the t quark dominates the mixing. This requires a numerical analysis to find how much the other terms contribute.

X. ISOSURFACES OF CONSTANT χ^2 IN THE 4×4 MATRIX PARAMETER SPACE

Here we examine the nine-angle-parameter space of the 4×4 down quark mixing matrix to find what the relationships between different angles are because of the constraints from all of the experiments. To do this we show the isosurfaces of constant χ^2 in three-dimensional subspaces of the nine-dimensional parameter space. (We can also show predictions for the FCNC transition amplitudes or for experiments on these isosurfaces by different colors or gray shadings.)

For the four parameters of the usual 3×3 CKM, $\theta_{12}(V_{us})$ is very well determined from V_{us} and V_{ud}, and we take only its central value here, since its variation has little effect on any of the other experiments. In the χ^2 we take from CLEO II [22,4]

$$|V_{ub}/V_{cb}| = 0.07 \pm 0.01, \tag{57}$$

$$|V_{cb}| = 0.043 \pm 0.007. \tag{58}$$

$\theta_{23}(V_{cb})$ and $\theta_{13}(V_{ub})$ are determined to about 17% and 21%, respectively. We vary these within 2σ of their central values. The angle, θ_{13} and phase δ_{13} are elements of $V_{ub} = s_{13}\exp(-i\delta_{13})$ and V_{td} and are often shown by ρ and η, where [23]

$$\rho + i\eta = V_{ub}^*/(|V_{cd}V_{cb}|) \simeq s_{13}\exp(i\delta)/(s_{12}s_{23}) \tag{59}$$

and

$$V_{td}/(|V_{cd}V_{cb}|) = 1 - \rho - i\eta. \tag{60}$$

δ_{13} and therefore ρ and η are not well determined [10,3] and FCNC limits on angles vary with these. Thus we are predominantly working in a space of three new angles and three phases with important variation. The calculations of χ^2 are carried out with a grid of seven points on the mixing angles and phases (sampling new phases at every 60° and δ_{13} about every 30°), and over a range of angles encompassing 2σ limits on the old angles and on the enclosing 2σ χ^2 range for the new angles.

Of the three-dimensional subspaces we show in Fig. 1 the $\chi^2 = 9.8$ isosurface corresponding to 2σ in the space of the three new mixing angles θ_{34} (up to 0.2), θ_{14} (up to 0.008), and θ_{24} (up to 0.03).

Considering the possibility of a nonzero value for U_{db} from B_d-$\bar{B}_d$ mixing through FCNC, from the form of Eq. (56), θ_{34} must be nonzero. Furthermore, for U_{db} to have a phase distinguishable from that of V_{td}^* which is in U_{db}'s first term in Eq. (56), and is the same phase as the standard model's contribution in Eq. (20), then θ_{14} or θ_{24} must also be nonzero. We find bounds on the new angles graphically by maximizing the extremes of the 2σ isosurface when varying the other angles and phases. The 2σ isosurfaces are all contained within the limits

$$\theta_{34} \leq 0.15, \quad \theta_{24} \leq 0.02, \quad \text{and} \quad \theta_{14} \leq 0.010. \tag{61}$$

These limits are then used in the calculations for maximum likelihood plots. While the limit on θ_{24} is about twice that on θ_{14}, the contribution of θ_{24} is reduced by s_{12} in U_{db}, Eq. (56). With these bounds and with $|V_{td}| \approx 0.01$ [3], the $s_{34}V_{td}^*$ term in U_{db}, Eq. (56) is smaller than the other two terms which bring in new phases and are large enough to make $|U_{db}| = 0.0007$ to account for B_d-$\bar{B}_d$ mixing.

XI. MAXIMUM LIKELIHOOD CORRELATION PLOTS BETWEEN STANDARD MODEL AND FCNC AMPLITUDES

In maximum likelihood correlation plots, we use for axes two output quantities which are dependent on the angles, such as $|U_{db}|$ and $|U_{\rm std}|$, and for each possible bin with given values for these, we search through the nine-dimensional angular data set and put in that bin the minimum χ^2 that gives the coordinates in the bin. We then draw contours at several χ^2 in this plane to present the results. This is a way to reduce the information from the nine-dimensional parameter space, and to give the likelihood for the important physically meaningful functions of the parameters. In general χ^2 is not a unique function of the two axis variables, but we do have a unique function to plot in terms of the minimum χ^2 or maximum likelihood.

The minimum χ^2 is found by computing over a grid of nine points in each angle covering the 2σ ranges for the standard mixing angles, and over the range found in the isosurface plots of the previous section for the new angles. The two new phases are covered in 30° grids, and δ_{13} in a 15° grid. The contribution of θ_{12} to χ^2 for the highly accurate $|V_{ud}|^2$ and $|V_{us}|^2$ experimental determinations can be treated analytically. The value of

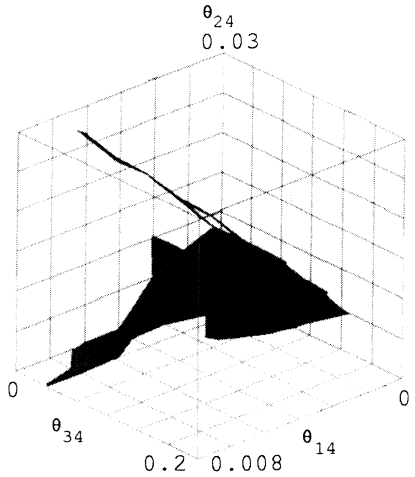

FIG. 1. The $\chi^2 = 9.8$ isosurface corresponding to 2σ in the space of the three new mixing angles to the fourth down quark, namely, θ_{34}, θ_{14}, and θ_{24}. The other mixing angles are at their central values, $\delta_{13} = 90°$, and the new phases are at zero.

θ_{12} that gives the minimum χ^2 for these two experiments is found analytically, and is effectively a function of θ_{34} since

$$|V_{ud}| \simeq \cos(\theta_{34})\cos(\theta_{12}), \tag{62}$$
$$|V_{us}| \simeq \cos(\theta_{34})\sin(\theta_{12}). \tag{63}$$

The other new angles are bounded to be too small to contribute in these two experiments. We use, for the experimental results and limits,

$$1 - |V_{ud}|^2 = 0.0505 \pm 0.0019, \tag{64}$$
$$|V_{us}|^2 = 0.0486 \pm 0.0008, \tag{65}$$
$$|V_{ub}|^2 \simeq 10^{-5}, \tag{66}$$
$$|V_{uD}|^2 = s_{14}^2 \leq 10^{-4}. \tag{67}$$

Varying θ_{12} to minimize the part of χ^2 from these two experiments gives s_{12} as a function of s_{34}:

$$s_{12}^2 = (0.0489 - 0.1506 s_{34}^2)/c_{34}^2. \tag{68}$$

This is then put back into χ^2 to get the minimum χ^2 from these two experiments. The small allowed variation of θ_{12} does not affect other experiments which have much larger uncertainties. The maximum likelihood plots are then contoured over a set of 15 × 15 bins.

We define the standard model amplitude for B_d-$\bar{B}_d$ mixing from Eq. (20) normalized so that it adds directly to U_{db}^2:

$$U_{\rm std}^2 \equiv \frac{\alpha}{4\pi \sin^2\theta_W} y_t f_2(y_t)(V_{td}^* V_{tb})^2, \tag{69}$$
$$x_d \propto |U_{\rm std}^2 + U_{db}^2|. \tag{70}$$

In Fig. 2(a), we show $|U_{db}|$ on the y axis and the standard model amplitude $|U_{\rm std}|$ on the x axis with contours at $\chi^2 = 4.7$, $\chi^2 = 9.8$, and $\chi^2 = 16.0$, which give the confidence levels corresponding to 1σ, 2σ, and 3σ, respectively. While $|U_{\rm std}|$ must be nonzero, we see that

$|U_{db}|$ can go from zero up to as large as the magnitude of $|U_{\rm std}|$ at a similar confidence level. In Fig. 2(b) is shown the analogous diagram for B_s-$\bar{B}_s$ mixing with a similar conclusion. Note the usual ratio of about 20 for $|U_{\text{std-}sb}|$ versus $|U_{\rm std}|$ which is about the ratio of $|V_{ts}|^2/|V_{td}|^2$.

We define the phases of the complete B_d-$\bar{B}_d$ amplitude $\phi_{\rm tot}$, the standard model amplitude $\phi_{\rm std} = 2\beta$, and their difference $\phi_{\rm diff}$ by

$$\phi_{\rm tot} = \arg(U_{\rm std}^2 + U_{db}^2), \tag{71}$$

$$\phi_{\rm std} = \arg(U_{\rm std}^2) = \arg[(V_{td}^* V_{tb})^2] = 2\beta, \tag{72}$$

$$\phi_{\rm diff} = \phi_{\rm tot} - \phi_{\rm std}. \tag{73}$$

The maximum likelihood plot for $\phi_{\rm tot}$ on the y axis and $\phi_{\rm std} = 2\beta$ on the x axis (using 20×20 bins) is shown in Fig. 3(a) for $m_t = 150$ GeV. The phase of B_d-$\bar{B}_d$ mixing enters into the CP-violating B decay asymmetries, such as in $B_d^0 \to J/\psi K_S$. We see that the phase of the total amplitude including FCNC and the standard model amplitude for B_d-$\bar{B}_d$ mixing at 1σ can range from $-90°$ to $180°$ while the standard model phases 2β ranges from $0°$ to $50°$. At 2σ the total amplitude can have any phase, while the standard model phase ranges from $-8°$ to $60°$. The analogous plot for B_s-$\bar{B}_s$ mixing, using analogous phases $\phi_{\text{tot}-sb}$ and $\phi_{\text{std}-sb} = \arg[(V_{ts}^* V_{tb})^2] = 2\beta_s$, is shown in Fig. 3(b). Here the phase of the total amplitude ranges over about $\pm 13°$ at 1σ while the standard model phase $2\beta_s$ is limited to about $\pm 5°$. At 2σ the total phase ranges to $\pm 26°$, while the standard model phase ranges up to about $\pm 6°$. $\beta_s = \arg(V_{ts}^* V_{tb})$ is the small angle from the b-s unitarity triangle which occurs in $b \to c\bar{c}s$ decays as $B_s \to \psi\phi$. In the standard model $\beta_s = \eta\lambda^2$ and is positive and about $1°$. Here with four down quarks, however, $V_{ts} \simeq (-s_{23} - s_{12}s_{13}\exp i\delta_{13} - s_{34}s_{24}\exp i\delta_{24})$ gets extra phases from the mixing angles to the fourth down quark and gives a larger and possibly negative phase to $U^2_{\text{std-}sb}$ corresponding to about $\pm 5°$ at 1σ.

We can also find a minimum χ^2 isosurface in a three-dimensional plot to elicit information on the interdependence and bounds on the three matrix elements at once, which we do in three orthogonal views in Fig. 4 to show the 1σ or $\chi^2 = 4.7$ isosurface in the space with axes $|V_{4d}|$, $|V_{4s}|$, and $|V_{4b}|$, that run from 0 to 0.02, 0.02, and 0.30, respectively. We see that at 1σ, the maximum likelihood

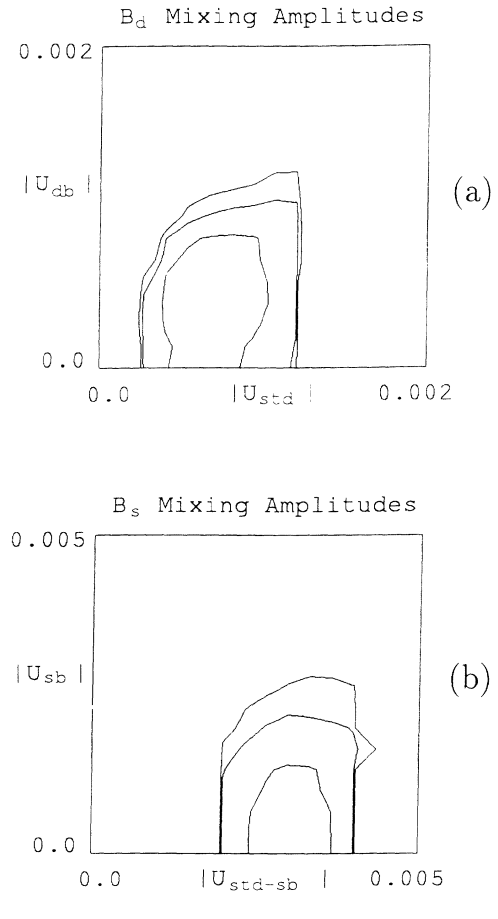

FIG. 2. (a) The maximum likelihood correlation plot between the FCNC amplitude for B_d-$\bar{B}_d$ mixing, $|U_{db}|$, and the standard model amplitude for the mixing, $|U_{\rm std}|$. The contours are at $\chi^2 = 4.7$, $\chi^2 = 9.8$, and $\chi^2 = 16.0$, corresponding to 1σ, 2σ, and 3σ, respectively. (b) The maximum likelihood plot for $|U_{sb}|$ versus $|U_{\text{std-}sb}|$ for B_s-$\bar{B}_s$ mixing.

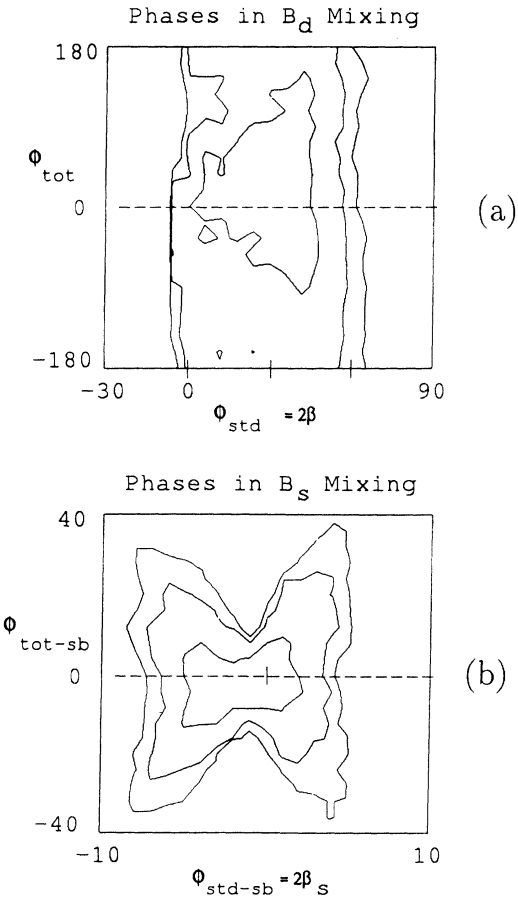

FIG. 3. Maximum likelihood correlation plot between the phase of the total amplitude $\phi_{\rm tot}$ and the standard model phase $\phi_{\rm std} = 2\beta$. Contours are at 1σ, 2σ, and 3σ for (a) B_d-$\bar{B}_d$ phases, and (b) B_s-$\bar{B}_s$ phases with a smaller range for $\phi_{\text{tot}-sb}$ and $\phi_{\text{std}-sb} = 2\beta_s$.

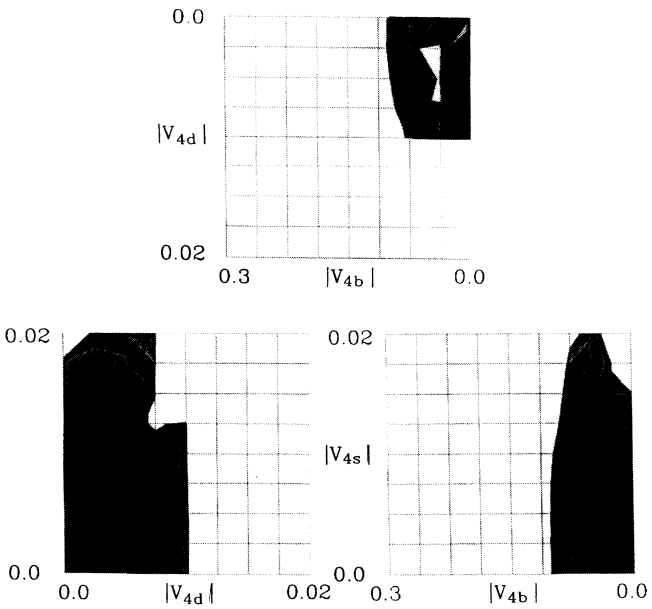

FIG. 4. Maximum likelihood correlation plot between the three new mixing matrix elements in the fourth row, $|V_{4d}|$, $|V_{4s}|$, and $|V_{4b}|$, showing the 1σ or $\chi^2 = 4.7$ isosurface in three orthogonal views. At the upper right is the top view with axes $|V_{4d}|$ and $|V_{4b}|$, on the left is the left side view with base $|V_{4d}|$ and height $|V_{4s}|$, and on the lower right is the right side view with base $|V_{4b}|$ and height $|V_{4s}|$.

bounds, searched over all angles, are

$$|V_{4d}| \leq 0.01, \quad |V_{4s}| \leq 0.02, \quad \text{and} \quad |V_{4b}| \leq 0.1. \quad (74)$$

XII. CORRECTIONS TO CKM UNITARITY TRIANGLES

The unitarity of the 4×4 mixing matrix requires orthogonality of the different rows. Instead of the three terms in the CKM orthogonality relation, which give a triangle in the complex plane, we now have four terms which give a quadrangle. The fourth terms are the $U_{ij} = -V_{4i}^* V_{4j}$ and the orthogonality relations are

$$U_{ds} = V_{ud}^* V_{us} + V_{cd}^* V_{cs} + V_{td}^* V_{ts}, \quad (75)$$

$$U_{sb} = V_{us}^* V_{ub} + V_{cs}^* V_{cb} + V_{ts}^* V_{tb}, \quad (76)$$

$$U_{db} = V_{ud}^* V_{ub} + V_{cd}^* V_{cb} + V_{td}^* V_{tb}. \quad (77)$$

In the unitarity triangle

$$\left| \frac{V_{ub} V_{ud}^*}{V_{cd}^* V_{cb}} \right| \simeq 0.32 \quad (78)$$

is the upper left-hand side. To this must be added the fourth side of

$$\left| \frac{U_{db}}{V_{cd}^* V_{cb}} \right| \leq 0.1, \quad (79)$$

which is at a barely detectable size. However, the upper

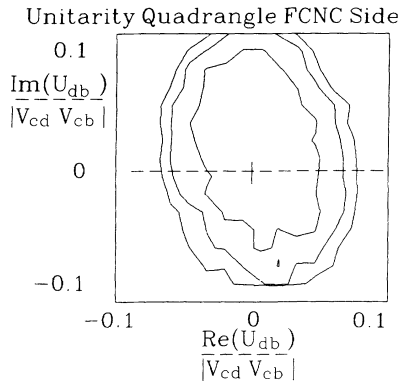

FIG. 5. Maximum likelihood plot for the contribution of the scaled FCNC amplitude $U_{db}/|V_{cd}^* V_{cb}|$ to the unitarity quadrangle, about the origin in the ρ-η plane, showing 1σ, 2σ, and 3σ contours. The dimensions are only 0.1 of the unit base of the unitarity quadrangle.

right-hand side proportional to $|V_{td}^* V_{tb}/V_{cd}^* V_{cb}|$ is heavily weighted against in the formula for B_d-$\bar{B}_d$ mixing, Eq. (20), and so U_{db} can still have an important contribution to the mixing and to its phase. In Fig. 5 is the maximum likelihood plot for the contribution of the scaled FCNC amplitude $U_{db}/|V_{cd}^* V_{cb}|$ as the fourth side of the unitarity quadrangle in the complex plane. The contours are at 1σ, 2σ, and 3σ. We see that the bound on $|U_{db}/V_{cd}^* V_{cb}|$ is roughly independent of direction, and bounded by 0.1.

XIII. *D* QUARK MASS AND PRODUCTION MECHANISMS

To estimate the new D quark mass, we use a Fritzsch ansatz relation between down quark mass ratios and mixing angles:

$$\theta_{34}^2 \simeq m_b/m_D. \quad (80)$$

The $|V_{4b}|$ mixing matrix element has the limit from Eq. (33) and from the χ^2 maximum likelihood isosurface plot, Fig. 4:

$$|V_{4b}| \simeq \theta_{34} \leq 0.1. \quad (81)$$

This gives a lower bound for m_D:

$$m_D \geq 100 \times m_b = 500 \text{ GeV}. \quad (82)$$

For production in an e^+-e^- collider, we note from Eq. (8) that the isovector coupling of the D quark to the Z^0 is suppressed by

$$(1 - |V_{44}|^2) \simeq |V_{4b}|^2 \leq 0.01, \quad (83)$$

and so the D singlet quark would be mainly produced by the photon and the electromagnetic part of the Z^0 current. At the 500 GeV mass it will have little influence on Z^0 parameters. Hadronically, it would be producible by gluon fusion, and the W fusion amplitude [from Eq. (2)] would be suppressed by $|V_{tD}|^2 = \theta_{34}^2 \leq 10^{-2}$.

XIV. CONCLUSIONS

Having formed a χ^2 for 13 experiments that constrain the 9 angles in the 4×4 down quark mixing matrix, we found ranges of the new mixing angles allowed by the constraints. We then studied the ranges and correlations of the magnitudes and phases of standard model amplitudes for B_d-$\bar{B}_d$ mixing with amplitudes including the flavor-changing neutral currents. We found that FCNC can contribute a significant part of B_d-$\bar{B}_d$ mixing and also B_s-$\bar{B}_s$ mixing. We also found that the phases of the total mixing amplitudes can differ from that of the standard model amplitudes by a large range of angles. These phases are those that are detected in B decay CP-violating asymmetries.

ACKNOWLEDGMENTS

This research was supported in part by the U.S. Department of Energy under Contract No. DE-FG03-91ER40679. We thank Professor David Cline, Professor William Molzon, and Professor Myron Bander for discussions, and Dr. Allen Schiano.

[1] P. Fishbane, S. Meshkov, R. E. Norton, and P. Ramond, Phys. Rev. D **31**, 1119 (1985); K. Enqvist, J. Maalampi, and M. Roos, Phys. Lett. B **176**, 396 (1986); A. Ray-Mukhopadhyaya and A. Raychaudhuri, Phys. Rev. D **37**, 807 (1988); G. Eilam and T. Rizzo, Phys. Lett. B **188**, 91 (1987); J. Maalampi and M. Roos, *ibid.* **188**, 487 (1987); J. Roldan, F. J. Botella, and J. Vidal, *ibid.* **283**, 389 (1992).

[2] M. Shin, M. Bander, and D. Silverman, Phys. Lett. B **219**, 381 (1989).

[3] D. Silverman, Phys. Rev. D **45**, 1800 (1992).

[4] W.-S. Choong and D. Silverman, Phys. Rev. D **49**, 1649 (1994).

[5] M. Kobayashi and T. Maskawa, Prog. Theor. Phys. **49**, 652 (1979).

[6] Y. Nir and D. Silverman, Nucl. Phys. **B345**, 301 (1990).

[7] T. Inami and C. S. Lim, Prog. Theor. Phys. **65**, 297 (1981).

[8] G. C. Branco, T. Morozumi, P. A. Parada, and M. N. Rebelo, Phys. Rev. D **48**, 1167 (1993).

[9] G. C. Branco, P. A. Parada, T. Morozumi, and M. N. Rebelo, Phys. Lett. B **306**, 398 (1993).

[10] F. Gilman and Y. Nir, Annu. Rev. Nucl. Part. Sci. **40**, 213 (1990).

[11] C. Albajar *et al.*, Phys. Lett. B **262**, 163 (1991).

[12] Y. Nir and D. Silverman, Phys. Rev. D **42**, 1477 (1990).

[13] A. Abada *et al.*, Nucl. Phys. **B376**, 172 (1992).

[14] A. Buras, Nucl. Phys. **B347**, 491 (1990); A. J. Buras and M. K. Harlander, in *Heavy Flavors*, edited by A. J. Buras and M. Linder (World Scientific, Singapore, 1992).

[15] G. Altarelli, R. Barbieri, and F. Caravaglios, Nucl. Phys. **B405**, 3 (1993), and updated in talk at Rencontres de la Vallee d'Aoste, La Thuile, Italy (unpublished); see also the analysis by L. Lavoura and J. P. Silva, Phys. Rev. D **47**, 1117 (1993).

[16] A. Schwartz, in *The Fermilab Meeting*, Proceedings of the Annual Meeting of the Division of Particles and Fields of the APS, Batavia, Illinois, 1992, edited by C. Albright *et al.* (World Scientific, Singapore, 1993); Princeton/HEP 92-15 KL-416. An earlier published value and description is in A. Heinson *et al.*, Phys. Rev. D **44**, 1 (1991).

[17] T. Akagi, Phys. Rev. Lett. **67**, 2618 (1991).

[18] C. Q. Geng and J. N. Ng, Phys. Rev. D **41**, 2351 (1990).

[19] F. J. Botella and L. L. Chau, Phys. Lett. **168B**, 97 (1986); H. Harari and M. Leuler, Phys. Lett. B **181**, 123 (1986).

[20] G. C. Branco and L. Lavoura, Nucl. Phys. **B278**, 738 (1986).

[21] A. B. Carter and A. I. Sanda, Phys. Rev. Lett. **45**, 952 (1980); Phys. Rev. D **23**, 1567 (1981); I. I. Bigi and A. I. Sanda, Nucl. Phys. **B193**, 85 (1981); **B281**, 41 (1987).

[22] P. Rankin, in "Proceedings of Aspen Winter Conference in Particle Physics," 1993 (unpublished); J. Bartelt *et al.*, Report Nos. CLNS93/1240, CLEO 93-15, 1993 (unpublished).

[23] L. Wolfenstein, Phys. Rev. Lett. **51**, 1945 (1983).

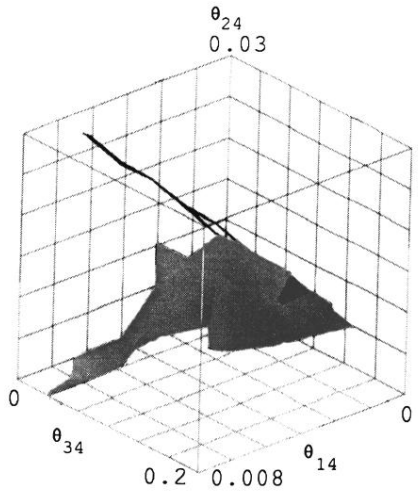

FIG. 1. The $\chi^2 = 9.8$ isosurface corresponding to 2σ in the space of the three new mixing angles to the fourth down quark, namely, θ_{34}, θ_{14}, and θ_{24}. The other mixing angles are at their central values, $\delta_{13} = 90°$, and the new phases are at zero.

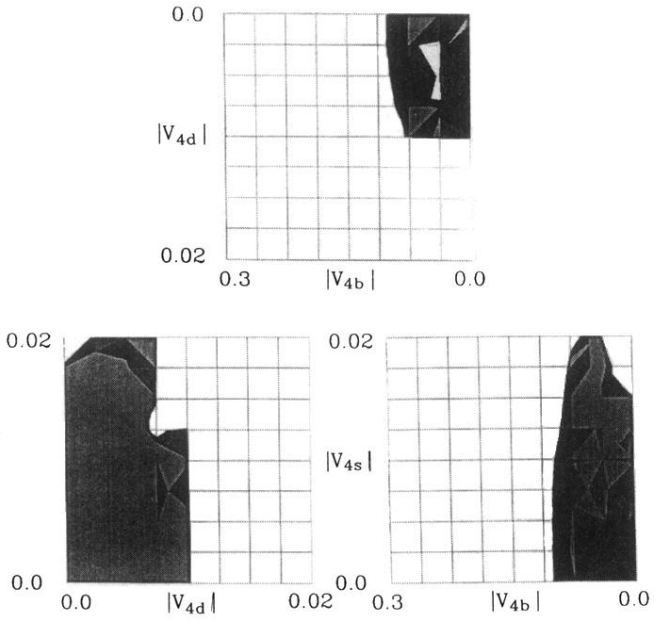

FIG. 4. Maximum likelihood correlation plot between the three new mixing matrix elements in the fourth row, $|V_{4d}|$, $|V_{4s}|$, and $|V_{4b}|$, showing the 1σ or $\chi^2 = 4.7$ isosurface in three orthogonal views. At the upper right is the top view with axes $|V_{4d}|$ and $|V_{4b}|$, on the left is the left side view with base $|V_{4d}|$ and height $|V_{4s}|$, and on the lower right is the right side view with base $|V_{4b}|$ and height $|V_{4s}|$.